International Journal of Aviation, Aeronautics, and Aerospace

Volume 8 | Issue 4 Article 6

2021

Design of a Laboratory Annular Combustor

Sathish Dharmalingam
RK University, Gujarat, India, research.sathish@gmail.com
Kartik Dolarkumar Kothari
RK University & Shree Hari Polytechnic Institute, Gujarat, India, kartikkothari8@gmail.com

The development of the jet engine and its associated components is advancing with the latest technologies in the industry (Bonser, 2019). The design of the combustor plays a vital role in power production and lowering emission levels. It is estimated that evolutionary technological improvements will save CO_2 emissions up to 30% by 2035 (Mathys et al., 2021). The combustor is the critical component in a gas turbine engine, through which the combustion of the air-fuel mixture takes place. The combustor is always installed in between the compressor and turbine. Annular, tubular, and tubo-annular are the three major configurations of combustor which are used for aero-engines. An annular combustor comprises an outer and inner liner, which are mounted concentrically inside an annular casing. An annular combustor provides more stable combustion with a lower pressure drop, and it is shorter in size with less surface area. Furthermore, this type of combustor provides uniform temperatures at the exit. Thus, the annular type of combustor is widely used among the tubular and tubo-annular types (Elhaj Mohammed, 2019). The various parts and zones of the annular combustor are shown in Figure 1. The practical experience and knowledge of designing the combustor are crucial for academic and research purposes on a laboratory-scale. Designing an annular combustor involves a rigorous iterative process, and there is no systematic procedure available to design a small-scale laboratory combustor used for research and academic purposes. The aim of the present work is to provide step-by-step procedures and concepts to aid the student, academician, or researcher in designing the laboratory scale annular combustor. The uniqueness of this research work is that it provides the entire calculation for all geometrical dimensions and the inclusiveness of the component-wise pressure drop factor for the complete design of an annular combustor.

The process flow of major design variables to design a laboratory scale annular combustor is shown in Figure 2. The design of the combustor must begin with local atmospheric data. The atmospheric data depends mainly on the altitude from the sea level at which the combustor is to be installed. The combustor presented here is designed for an altitude of $102\ m$ above sea level. The standard atmospheric pressure, density, and temperature for this altitude are measured to be $98.9\ kpa$, $1.213\ kg/m^3$, and $298\ K$ respectively. For lab-based small gas turbine combustors, the compressor is not employed, whereas air from the air-compressor or blower has been used. Here, a blower with a volume flow rate of $3.5\ m^3/min$ is chosen, and thus, the mass flow rate of air ($\dot{m}_3$) at the inlet is $0.06701\ kg/s$. The inlet air temperature (T_3) is $298\ K$.

Figure 1

Schematic of the Annular Combustor

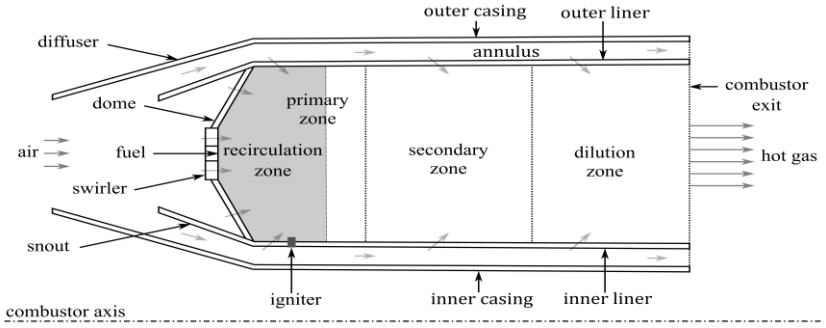

Figure 2

Process Flow of Design Calculation

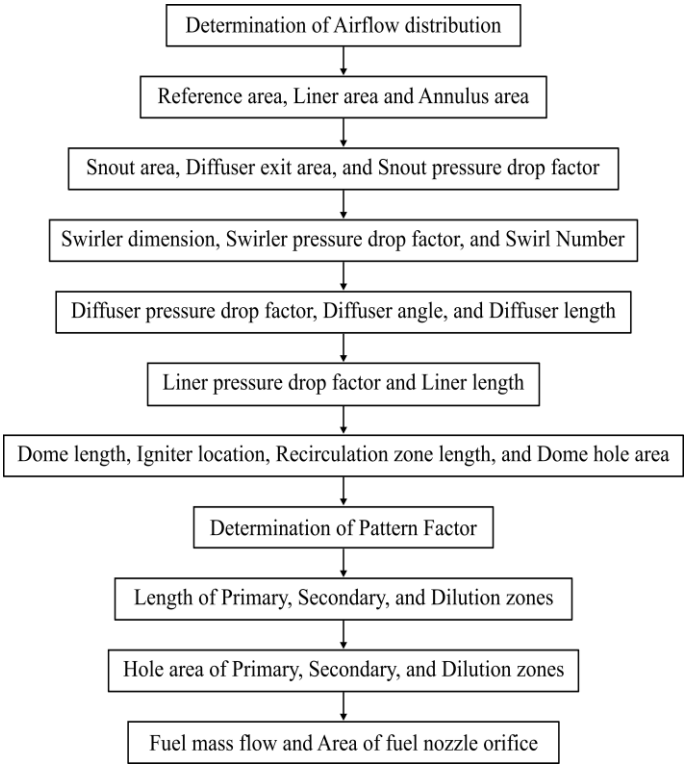

Airflow Distribution

The airflow distribution depends upon the air inlet conditions and the turbine requirements. About half of the primary zone air mass flow rate can be admitted through the swirler and as dome cooling in the case of conventional design (Rolls Royce, 1996).

The mass flow rate at the recirculation zone ($\dot{m}_{rz}$) is the sum of the air entered into the primary zone through the swirler ($\dot{m}_{sw}$) and the air admitted through dome cooling slots ($\dot{m}_{do}$). That is,

$$\dot{m}_{rz} = \dot{m}_{sw} + \dot{m}_{do} \tag{1}$$

The remaining air is fed through the annulus ($\dot{m}_{an}$) and it is distributed to the primary, secondary, and dilution zones as per the combustor specification. The mass flow rate through the swirler has to be available in a quantity that should provide an equivalence ratio greater than 1 for ignition and flame stability at the primary zone of the combustor. However, the equivalence ratio at the recirculation zone must not exceed 1.5 to minimize smoke formation and the emission of carbon monoxide and unburned hydrocarbons in the product gases. Liner cooling is essential for the conventional combustor to prevent the liner from melting down at higher temperatures. The percentage of cooling air from the core air mass flow has to be distributed along the zones (Odgers, 1977).

$$cooling\ air\ \% = 0.1 \times T_3 - 30 \tag{2}$$

However, for a small-scale lab-based research combustor, the air inlet temperature is typically low at around $300\ K$. Substituting this value in Eq.(2) will give zero, and thus a lab-based combustor operating at a low inlet temperature typically does not require liner cooling. In the present design, it is decided that 20% of $\dot{m}_3$ is to be admitted to the recirculation zone through swirler and dome cooling holes, and 20%, 25%, and 35% of $\dot{m}_3$ are to be admitted to the primary, secondary, and dilution zone through the annulus, respectively. However, this percentage can be varied according to the combustor specification and turbine requirements. The complete airflow distribution is shown in Table 1.

Table 1
Air Mass Flow Distribution in Percentage

Inlet ($\dot{m}_3$) 100%	Recirculation zone/Snout ($\dot{m}_{rz}$) 20%	Swirler ($\dot{m}_{sw}$) 10%
		Dome cooling ($\dot{m}_{do}$) 10%
	Annulus ($\dot{m}_{an}$) 80%	Primary zone ($\dot{m}_{pz}$) 20%
		Secondary zone ($\dot{m}_{sz}$) 25%
		Dilution zone ($\dot{m}_{dz}$) 35%

Initial Sizing

Combustor sizing has to be carried out after the determination of air mass flow distribution, and the schematic of combustor sizing is shown in Figure 3. The reference area (A_{ref}) without the liner thickness can be calculated from Eq.(3) (Conrado et al., 2004).

$$A_{ref} = \frac{\pi}{4}\left[\left(2 \times D_{ref} + D_{ic}\right)^2\right] - \frac{\pi}{4}D_{ic}^2 \quad (3)$$

where D_{ref} is the half-reference diameter and D_{ic} is the inner casing's outer diameter.

Figure 3
Combustor Sizing

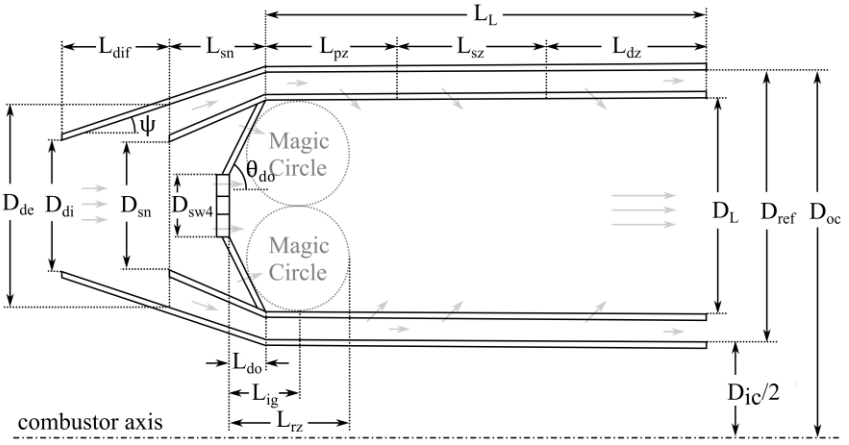

However, the practical combustor always has a thickness, and hence the reference area (A_{ref}) for the annular combustor with a thickness can be calculated using Eq.(4)

$$A_{ref} = \frac{\pi}{4}\left[\left(2 \times D_{ref} + D_{ic}\right)^2\right] - \frac{\pi}{4}D_{ic}^2 - \frac{\pi}{4}(2 \times D_t)^2 \quad (4)$$

where D_t is the sum of the outer and inner liner thicknesses. Let us assume the initial values of the outer casing and inner casing have sufficient thickness as per the requirement. In this present design, D_{ref} and D_{ic} are taken as $0.06\ m$ and $0.04\ m$, respectively.

$$\begin{aligned} A_{ref} &= \frac{\pi}{4}[(2 \times 60 \times 10^{-3} + 40 \times 10^{-3})^2 - (40 \times 10^{-3})^2 \\ &\quad - (2 \times 2 \times 10^{-3})^2] \\ &= 11259.46802 \times 10^{-6}\ m^2 \end{aligned} \quad (5)$$

The combustor liner area (A_L) should be 0.65 to 0.67 times that of A_{ref} for a quality design of an annular combustor (Melconian & Modak, 1985). The sectional length, D_L, can be obtained from the value of A_L.

$$\begin{aligned} A_L &= 0.667 \times A_{ref} \\ &= 7510.0652\ \times 10^{-6}\ m^2 \end{aligned} \quad (6)$$

We know that,

$$A_L = \frac{\pi}{4}(2 \times D_L)^2 \quad (7)$$

Thus,

$$D_L \approx 0.049\ m \quad (8)$$

The annulus area (A_{an}) is the difference between A_{ref} and A_L (Mark & Selwyn, 2016) and can be calculated from Eq.(9).

$$\begin{aligned} A_{an} &= A_{ref} - A_L \\ &= 3749.4\ \times 10^{-6}\ m^2 \end{aligned} \quad (9)$$

Snout

The purpose of the snout is to regulate the airflow from the diffuser toward the recirculation zone. Eq.(10) is used for calculating the cross-sectional area of the diffuser at which the snout inlet plane exists (A_{de}) or the cross-sectional area of the snout inlet (A_{sn}) (Sawyer, 1985).

$$\frac{A_{sn}}{A_{de}} = \frac{\dot{m}_{sn}}{\dot{m}_3} \times \frac{1}{C_{ds}} \quad (10)$$

where C_{ds} is the snout discharge coefficient, and for a uniform compressor/air delivery, this approaches unity. For conventional combustor snouts, the mass flow rate is approximately equal to half of the primary zone airflow. Here, 20% of air is admitted into the primary zone through the annulus, and 20% of air is admitted into the recirculation zone through the dome and

swirler. Notice that the recirculation zone is a part of the primary zone. Thus, 40% of total air mass flow is admitted to the primary zone, and hence, 50% of this primary airflow (i.e., 20%) may be allowed through the snout. The snout mass flow will vary with snout area, diffuser configuration, and total inlet air mass flow. Here, A_{sn} is calculated using Eq.(11), assuming a reasonable value for the snout diameter (D_{sn}), so that A_{de} can be found using Eq.(10).

$$A_{sn} = \frac{\pi}{4}(2 \times D_{sn})^2 = 1256.63706 \times 10^{-6}\, m^2 \quad (11)$$

Rearranging the Eq.(10)

$$A_{de} = \frac{A_{sn} \times \dot{m}_3 \times C_{ds}}{\dot{m}_{sn}} = 6283.1853 \times 10^{-6}\, m^2 \quad (12)$$

We know that,

$$A_{de} = \frac{\pi}{4}(2 \times D_{de})^2 \quad (13)$$

Thus, the diameter of the diffuser at which the snout inlet plane exists is

$$D_{de} = 44.72136 \times 10^{-3}\, m \quad (14)$$

Snout Pressure Drop Factor

The airflow from the compressor or blower is directed to the recirculation zone through the snout, and the remaining air is directed to the combustion volume through the annulus. The swirler and dome are installed inside the snout. The geometry of the snout, diffuser, and reference area (A_{ref}) are the factors affecting the snout pressure drop factor. A larger reference area is demanded by higher snout pressure drops. Thus, the combustor volume will become larger, and hence the snout pressure drop should be optimum. The snout pressure drop factor is calculated from Eq.(15) (Saboohi et al., 2016).

$$\frac{\Delta p_{sn}}{q_{ref}} = 0.25 \times \frac{q_{sn}}{q_{ref}} = 0.25\left(\frac{A_{ref}}{A_{de}}\right) = 0.448 \quad (15)$$

Swirler

A swirler imparts a swirl to the airflow by converting the axial airflow to tangential ones for better air-fuel mixing. This tangential airflow produces a flow recirculation which takes the hot gases back to the flame front, preventing the flame blow-off and thereby increasing the flame stability. Thus, the main role of the swirler is to enhance the mixing quality of the air-fuel mixture, while the toroidal motion of the flow reduces the flame length also (Chen & Driscoll, 1989). The swirler area can be calculated using Eq.(16) (Knight & Walker, 1953).

$$\frac{\Delta p_{sw}}{q_{ref}} = K_{sw}\left[\left(\frac{A_{ref}}{A_{sw}}\right)^2 sec^2\beta_{sw} - \left(\frac{A_{ref}}{A_L}\right)^2\right] \times \left(\frac{\dot{m}_{sw}}{\dot{m}_3}\right)^2 \quad (16)$$

where β_{sw} is the turning angle of the airflow, it ranges from 30^o to 60^o (Mellor, 1990). The swirler discharge parameter K_{sw} is 1.30 for thin straight blades and 1.15 for thin curved blades (Saboohi et al., 2016). The physical flow area of the swirler is the annulus area corrected for the swirl and flow blockage by vanes, and it is calculated using Eq.(17) (Khandelwal et al., 2014; Mellor, 1990). The vane thickness (v_t) is to be assumed and the range is from $0.7\,mm$ to $1.5\,mm$ (Mellor, 1990), and here $1\,mm$ is chosen based on manufacturing constraints. The number of vanes (n_v) is to be assumed, and the range is from 8 to 16 (Mellor, 1990). For a small research-based laboratory combustor, $n_v = 8$ is sufficient to avoid more blockage to the airflow. Experiments had shown that the combustors performed well for $\dot{m}_{sw}$ ranging from 3% to 12% of the total air $(\dot{m}_3)$ and $8 - 10$ blades (Conrado et al., 2004). The dimensions of the swirler are shown in Figure 4.

$$A_{sw} = \frac{\pi}{4} \times (D_{sw3}^2 - D_{sw2}^2) - 0.5 \times n_v \times v_t(D_{sw3} - D_{sw2})$$
$$= 485.48667 \times 10^{-6}\, m^2 \quad (17)$$

Figure 4

Dimensions of Swirler

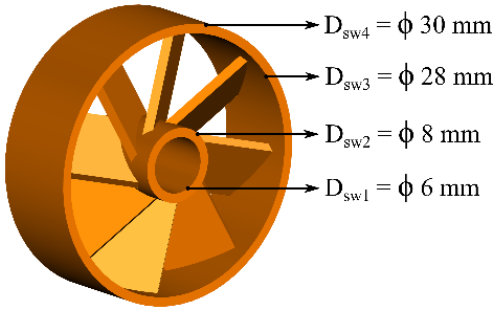

Swirler Pressure Drop Factor

The factors affecting the swirler pressure drop are the swirler area, blade turning angle, swirler discharge parameter, reference area, and the liner area. A swirler pressure drop factor can be obtained by substituting all the known values in Eq.(16).

$$\frac{\Delta p_{sw}}{q_{ref}} = 1.3 \times \left[\left(\frac{11259.46802 \times 10^{-6}}{485.48667 \times 10^{-6}}\right)^2 sec^2 42^o - \left(\frac{11259.46802 \times 10^{-6}}{7510.0652 \times 10^{-6}}\right)^2\right] \times \left(\frac{0.6701 \times 10^{-2}}{6.701 \times 10^{-2}}\right)^2 = 12.632 \quad (18)$$

Swirl Number

The Central Recirculation Zone (CRZ) is essential for anchoring the flame, better air-fuel mixing, and the continuous source of ignition (Mohammad & Jeng, 2009). A low swirl number leads to a lower residence time of the reactive mixture in the primary zone. A higher swirl number improves the air-fuel mixing and an increase in the residence time of the combustion products, leads to more efficient combustion. However, as the swirl number increases, so does NO_X emission (Lokini et al., 2019). The swirl number greater than 0.6 is expected for better flow recirculation (Mattingly et al., 2002) and the setup of the Central Recirculation Zone (CRZ) in the combustor. Hence, it is considered that the swirl motion is sufficient when the swirl number is larger than 0.6 (Hayakawa et al., 2017; Lefebvre & Ballal, 2010; Syred & Beér, 1974). The swirl number (S_N) is calculated from Eq.(19) (Saboohi et al., 2016).

$$S_N = \frac{2}{3}\tan\beta_{sw}\frac{1-(D_{sw2}/D_{sw3})^3}{1-(D_{sw2}/D_{sw3})^2} = 0.63892 \quad (19)$$

The achieved swirler number satisfies the expected value, and that confirms the setup of CRZ in the combustor.

Design of the Diffuser

The swirler pressure drop factor, combustor total pressure drop factor, and snout pressure drop factor must be known to calculate the diffuser pressure drop factor and are calculated using Eq.(20) (Saboohi et al., 2016).

$$\frac{\Delta p_{dif}}{q_{ref}} = \frac{\Delta p_{3-4}}{q_{ref}} - \frac{\Delta p_{sw}}{q_{ref}} - \frac{\Delta p_{sn}}{q_{ref}} = 6.92 \quad (20)$$

The diffuser angle can be found using Eq.(21) (Mark & Selwyn, 2016).

$$\psi = tan^{-1}\left[\frac{\frac{\Delta p_{dif}}{p_3} \times {A_{di}}^2 \times {p_3}^2}{502.4 \times \left(1 - \frac{A_{di}}{A_{de}}\right)^2 \times {\dot{m}_3}^2 \times T_3}\right]^{1/1.22} \quad (21)$$

Alternatively, for maintaining a constant angle from the diffuser inlet to the outer casing of the combustor, Eq.(22) can be used. D_{di} is the diffuser inlet diameter and is the exit diameter of the compressor. As described earlier, for a small gas turbine combustor, usually an air compressor or blower has been used. In such cases, D_{di} can be taken as the exit diameter of the air compressor/blower extension pipe. Assuming the length of the snout (L_{sn}), the length of the diffuser can be found.

$$\begin{aligned} L_{dif} &= \frac{(D_{de} - D_{di})}{(D_{oc} - D_{de})} \times L_{sn} \\ &= 0.02914032\ m \end{aligned} \quad (22)$$

Liner Length

The liner length (L_L) depicts the total length of the zones, i.e., the sum of primary, secondary, and dilution zone lengths. The pressure drop across the liner (Δp_L) needs to be known to determine the liner length. The pressure drop across the liner can be found using Eq.(23) (Lefebvre & Ballal, 2010).

$$\begin{aligned} \frac{\Delta p_L}{q_{ref}} &= \frac{\Delta p_{3-4}}{q_{ref}} - \frac{\Delta p_{dif}}{q_{ref}} \\ &= 13.08 \end{aligned} \quad (23)$$

Notice that the liner pressure drop factor $\left(\frac{\Delta p_L}{q_{ref}}\right)$ is approximately equal to the swirler pressure drop factor $\left(\frac{\Delta p_{sw}}{q_{ref}}\right)$ (Mohammad & Jeng, 2009). Usually, the liner pressure drop should be $60 - 70\%$ of the total pressure drop through the combustor (Mellor, 1990; Mohammad & Jeng, 2009), and here 65.4% of the total pressure drop is achieved. The liner length, $L_L = (0.25 \sim 0.35) \times D_{ref}$ (Zhang et al., 2019), and is calculated as in Eq.(24).

$$\begin{aligned} L_L &= 0.35 \times D_{ref} \\ &= 0.021\ m \end{aligned} \quad (24)$$

Dome and Igniter

Dome angle influences the recirculation of reactive mixture and product gases, which also affects the hot spot zones and flame stabilization in the upstream portion of the primary zone (Kim et al., 2009). For the conventional

combustor, the dome angle (θ_{do}) is kept at around 60^o. Thus, the dome length can be found as in Eq.(25) (Saboohi et al., 2016).

$$\begin{aligned} L_{do} &= \frac{D_L - D_{sw4}}{2 \times \tan(\theta_{do})} \\ &= \frac{0.049 - 0.030}{2 \times \tan 60^o} \\ &= 0.005484\ m \end{aligned} \tag{25}$$

The igniter must be placed in a predicted position at which the fresh air-fuel mixture is rich. The location where the magic circles touch the liner wall is proposed for the quoted feature.

$$\begin{aligned} L_{ig} &= \frac{D_L}{4}\left[1 + cot\left(\frac{\pi - \theta_{do}}{2}\right)\right] + L_{do} - \frac{D_L}{4} \\ &= 0.01255\ m \end{aligned} \tag{26}$$

The recirculation zone length is given by Eq.(27) (Saboohi et al., 2016).

$$\begin{aligned} L_{rz} &= L_{ig} + \frac{D_L}{4} \\ &= 0.0248\ m \end{aligned} \tag{27}$$

Air can be admitted through holes or slots in the dome section apart from the swirler. To avoid complexity in mounting and installation, it is always preferred to have holes instead of slots for small combustor designs. In this current design, 10% of total air mass flow ($\dot{m}_3$) from the air-compressor or blower is admitted through the dome section into the combustor recirculation zone, as given in Table 1. Due to the discharge coefficient, the air jet area is always less than the geometric area. The geometric area of the hole (Lefebvre & Ballal, 2010) can be calculated if the pressure difference across the dome is known or assumed. The coefficient of discharge, $C_D = 0.6$ (Lefebvre & Ballal, 2010), is taken for the simple circular hole.

$$\begin{aligned} \dot{m}_{do} &= C_D \times A_{geo}[2 \times \rho_3(p_u - p_d)]^{0.5} \\ A_{geo} &= 3.1415927 \times 10^{-4}\ m^2 \end{aligned} \tag{28}$$

where ρ_3 is the inlet air density, p_u and p_d are the upstream and downstream pressures of the dome, respectively. The number of holes depends on the size and space availability of the dome for the equal distribution of air. The air admitted to the dome not only contributes to the dome cooling, but it can also assist the air-fuel mixing to some extent, along with the swirler. Here, sixteen holes are planned for air admission. Thus, $1.963495 \times 10^{-5}\ m^2$ is the required area for each hole. The geometric diameter of each hole can be calculated using Eq.(29).

$$d_{gh} = \left[\frac{4 \times A_{geo}}{\pi}\right]$$

$$= 5 \times 10^{-3}\, m \tag{29}$$

Determination of Pattern Factor

The Pattern Factor (PF) provides the temperature distribution of the combusted gases across the radial and circumferential directions at the exit of the combustor. The pattern factor for the present annular combustor is calculated using Eq. (30) (Lefebvre & Ballal, 2010).

$$PF = \frac{T_{max} - T_4}{T_4 - T_3} = 1 - exp\left[-0.05 \times \frac{L_L}{D_L} \times \frac{\Delta p_L}{q_{ref}}\right]^{-1} \approx 0.30 \tag{30}$$

where T_{max} is the maximum recorded temperature, T_4 is the mean exit temperature, and T_3 is the inlet air temperature. Contemporary main burners exhibit PF ranging from $0.25 - 0.45$. $PF \approx 0.30$ falls within the acceptable range.

Zone Length

The liner length is divided into primary, secondary, and dilution zones. The zone in which the primary air is admitted via liner holes is termed the "primary zone." The purpose of the primary zone is to develop the highest possible temperature for the high-speed reaction or rate of flame propagation. The primary zone needs to be operated at the stoichiometric mixture ratio. It is usual to allow some air as secondary air to promote the proper mixing of air and fuel and ensures the required oxygen for the given fuel supply for complete combustion. The secondary air is admitted via liner holes, and this zone is termed the "secondary zone." The dilution air is admitted to bring down the gas temperature to the required Turbine Inlet Temperature (TIT). The zone in which the dilution air is admitted via dilution holes is called the "dilution zone." The zone length is majorly dependent on the reference diameter, liner diameter, and pattern factor.

Primary Zone Length

The length of the primary zone, $L_{pz} = (0.9{\sim}1.5) \times D_{ref}$ (Zhang et al., 2019), and can be calculated in Eq.(31).

$$L_{pz} = 1.1 \times D_{ref} = 0.066\, m \tag{31}$$

Dilution Zone Length

The length of the dilution zone can be calculated using Eq.(32) (Melconian & Modak, 1985).

$$\begin{aligned} L_{dz} &= D_L(3.83 - 11.83 \times PF + 13.4 \times PF^2) \\ &= 0.072863\, m \end{aligned} \tag{32}$$

Secondary Zone Length

The length of the secondary zone can be calculated using Eq.(33).

$$L_{sz} = L_L - L_{pz} - L_{dz} = 0.071748\ m \tag{33}$$

Liner Holes

The reference dynamic pressure (q_{ref}) is required to calculate the pressure drop across the liner. Reference Velocity (v_{ref}) can be calculated as in Eq.(34) (Lefebvre & Ballal, 2010).

$$\begin{aligned} v_{ref} &= \frac{\dot{m}_3}{\rho_3 \times A_{ref}} \\ &= \frac{0.06701}{1.213 \times 11259.46802 \times 10^{-6}} \\ &= 4.906377\ m/s \end{aligned} \tag{34}$$

The reference dynamic pressure (q_{ref}) can be calculated as in Eq.(35) (Lefebvre & Ballal, 2010).

$$\begin{aligned} q_{ref} &= \frac{\rho_3 \times {v_{ref}}^2}{2} \\ &= \frac{1.213 \times 4.906377^2}{2} \\ &= 14.5997129\ kg/m - s^2 \end{aligned} \tag{35}$$

Thus, from Eq.(23)

$$\begin{aligned} \Delta p_L &= 13.08 \times q_{ref} \\ &= 190.96424\ pa \end{aligned} \tag{36}$$

Primary Zone Holes

The number of holes required in total for both the outer and inner liner in the primary zone (n_{pz}) can be calculated using Eq.(37) (Lefebvre & Ballal, 2010).

$$\begin{aligned} n_{pz} \times {d_{jpz}}^2 &= \frac{4 \times \dot{m}_{pz}}{\pi \times (2 \times \Delta p_L \times \rho_3)^{0.5}} \\ &= 7.927902 \times 10^{-4} \end{aligned} \tag{37}$$

For $d_{jpz} = 4 \times 10^{-3}\ m$,

$$n_{pz} \approx 50 \tag{38}$$

The actual geometric diameter of primary zone holes (d_{hpz}) is then given by Eq.(39) (Lefebvre & Ballal, 2010).

$$d_{hpz} = \frac{d_{jpz}}{{C_D}^{0.5}}$$

$$= 5.163 \times 10^{-3}\ m \tag{39}$$

Secondary Zone Holes

The number of secondary zone holes (n_{sz}) required in total for both the outer and inner liner can be calculated using (40) (Lefebvre & Ballal, 2010).

$$n_{sz} \times {d_{jsz}}^2 = \frac{4 \times \dot{m}_{sz}}{\pi \times (2 \times \Delta p_L \times \rho_3)^{0.5}} = 9.9106568 \times 10^{-4} \tag{40}$$

For $d_{jsz} = 6 \times 10^{-3}\ m$,

$$n_{sz} \approx 28 \tag{41}$$

The actual geometric diameter of secondary zone holes (d_{hsz}) is then given by Eq.(42) (Lefebvre & Ballal, 2010).

$$d_{hsz} = \frac{d_{jsz}}{{C_D}^{0.5}} = 7.745 \times 10^{-3}\ m \tag{42}$$

Dilution Zone Holes

The number of holes required in total for both the outer liner and inner liner in the dilution zone (n_{dz}) can be calculated using Eq.(43) (Lefebvre & Ballal, 2010)**.**

$$n_{dz} \times {d_{jdz}}^2 = \frac{4 \times \dot{m}_{dz}}{\pi \times (2 \times \Delta p_L \times \rho_3)^{0.5}} = 13.873829 \times 10^{-4} \tag{43}$$

For $d_{jdz} = 8 \times 10^{-3}\ m$,

$$n_{dz} \approx 22 \tag{44}$$

The actual geometric diameter of dilution zone holes (d_{hdz}) is then given by Eq.(45) (Lefebvre & Ballal, 2010).

$$d_{hdz} = \frac{d_{jdz}}{{C_D}^{0.5}} = 10.327 \times 10^{-3}\ m \tag{45}$$

The primary, secondary, and dilution holes are made with staggered arrangements for better airflow distribution and to avoid local hotspots.

Fuel Flow Distribution

Liquified Petroleum Gas (LPG) is chosen as the fuel, as it is readily available and safe to handle compared to liquid fuels. The mass flow rate of air is $6.701 \times 10^{-2}\ kg/s$, and the stoichiometric air-fuel ratio (AF_{stoi}) is 15.46, so the mass flow rate of fuel can be calculated using Eq.(46).

$$\dot{m}_f = \frac{\dot{m}_a}{AF_{stoi}} = 4.334 \times 10^{-3}\ kg/s \quad (46)$$

A simple, plain orifice fuel nozzle is used. The coefficient of discharge of a plain orifice nozzle can be varied depending on its length-diameter ratio (Lefebvre & Ballal, 2010). The density of LPG is $2.469135\ kg/s$ (can be varied with chemical composition), then the geometric area of the nozzle orifice (Lefebvre & Ballal, 2010) can be found if the pressure difference across the orifice is known.

$$\dot{m}_f = C_D \times A_{geo}\left[2 \times \rho_{lpg}\left(p_1 - p_j\right)\right]^{0.5}$$
$$A_{geo} = 1.0058571 \times 10^{-4}\ m^2 \quad (47)$$

where p_1 is the upstream fuel pressure and p_j is the fuel jet pressure coming out of the orifice. The number of the fuel nozzles depends on the size and space availability of the combustor for the equal distribution of fuel. Here, eight fuel nozzles are planned for fuel admission. Thus, $1.257321 \times 10^{-5}\ m^2$ is the required area of each fuel nozzle orifice. Thus, the geometric diameter of each orifice $\left(d_{gn}\right)$ can be calculated using Eq.(48).

$$d_{gn} = \left[\frac{4 \times A_{geo}}{\pi}\right] = 4 \times 10^{-3}\ m \quad (48)$$

The final dimensions of a small-scale laboratory annular combustor are shown in Figure 5. The CAD model of the combustor assembly and its cutaway are shown in Figures 6 and 7, respectively.

Figure 5

A Sectional View of the Combustor Assembly

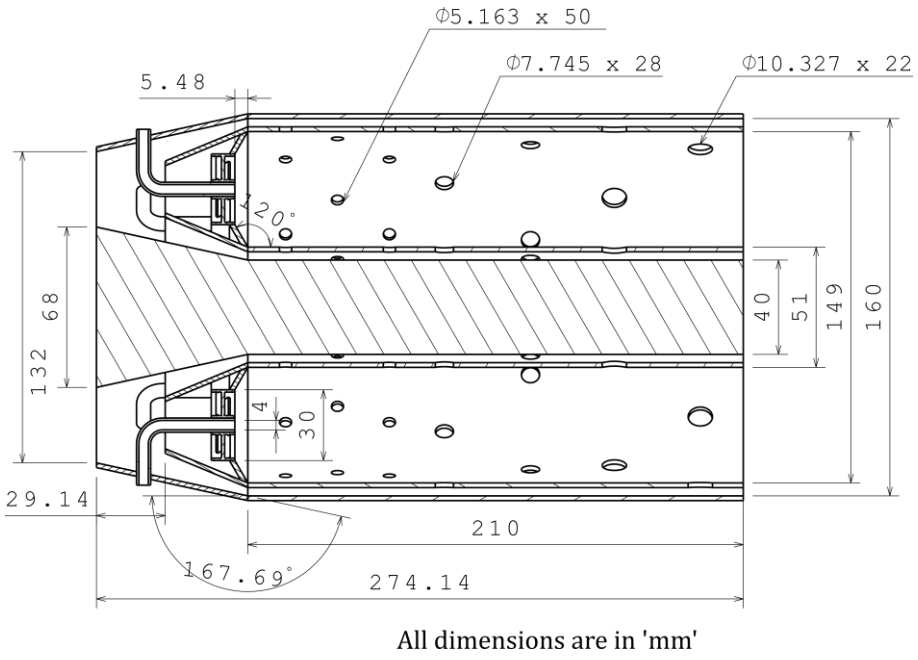

Figure 6

Assembly of an Annular Combustor

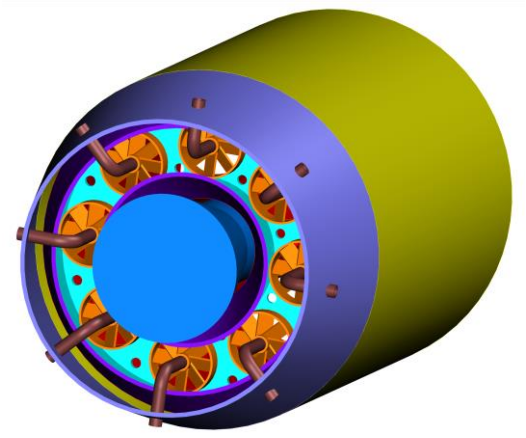

Figure 7

Cutaway of the Combustor Assembly

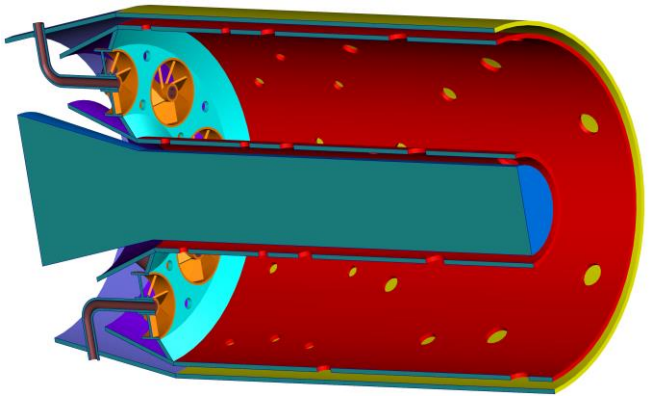

Conclusion

A systematic procedural design of a small-scale annular combustor was presented. The procedure starts with atmospheric data for the altitude at which the combustor needs to be installed. The airflow distribution was decided based on swirler mass flow and dome cooling, which affect the equivalence ratio at the recirculation zone. The airflow distribution depends on cooling airflow, and here, due to the absence of cooling airflow, the air mass flow was shared between the secondary and the dilution zone. It is observed that the snout pressure drop factor is very small compared to other pressure drop factors. The achieved swirler number satisfies the expected value and confirms the setup of CRZ. The achieved liner pressure drop factor is approximately equal to the swirler pressure drop factor, which confirms the accuracy of the design. Usually, the liner pressure drop should be $60 - 70\%$ of the total pressure drop through the combustor, and here 65.4% of the total pressure drop is achieved. Contemporary main burners exhibit pattern factors ranging from 0.25 to 0.45, and the pattern factor of the present design is 0.30, falling within the acceptable range. All calculated values confirm the perfect design of a small-scale laboratory annular combustor. The design procedure shown here is a preliminary concept, and future work will include more study. With the help of this procedural design, any student, academician, or researcher can easily design the laboratory scale annular combustor. Furthermore, this design can be validated using a Computational Fluid Dynamics (CFD) simulation, and then the experimental studies can be performed.

https://commons.erau.edu/ijaaa/vol8/iss4/6
DOI: https://doi.org/10.15394/ijaaa.2021.1647

References

Bonser, M. P. (2019). Global aviation system: Towards sustainable development. *International Journal of Aviation, Aeronautics, and Aerospace*, *6*(3). https://doi.org/10.15394/ijaaa.2019.1356

Chen, R. H., & Driscoll, J. F. (1989). The role of the recirculation vortex in improving fuel-air mixing within swirling flames. *22nd International Symposium on Combustion, The Combustion Institute, Elsevier*, *22*(1), 531–540. https://doi.org/10.1016/S0082-0784(89)80060-8

Conrado, A. C., Lacava, P. T., Filho, A. C. P., & Sanches, M. de S. (2004). Basic design principles for gas turbine combustor. *Proceeding of 10th Brazillian Congress of Thermal Sciences and Engineering, Braz. Soc. of Mechanical Sciences and Engineering - ABCM, Brazil*, 1–12.

Elhaj Mohammed, R. S. (2019). Design and analysis of annular combustion chamber for a micro turbojet engine. *International Journal of Aerospace and Mechanical Engineering, International Scholarly and Scientific Research & Innovation*, *13*(4), 282–287.

Hayakawa, A., Arakawa, Y., Mimoto, R., Somarathne, K. D. K. A., Kudo, T., & Kobayashi, H. (2017). Experimental investigation of stabilization and emission characteristics of ammonia/air premixed flames in a swirl combustor. *International Journal of Hydrogen Energy*, *42*(19), 14010–14018. https://doi.org/10.1016/j.ijhydene.2017.01.046

Khandelwal, B., Lili, D., & Sethi, V. (2014). Design and study on performance of axial swirler for annular combustor by changing different design parameters. *Journal of the Energy Institute*, *87*(4), 372–382. https://doi.org/10.1016/j.joei.2014.03.022

Kim, H. S., Arghode, V. K., & Gupta, A. K. (2009). Combustion characteristics of a lean premixed LPG–air combustor. *International Journal of Hydrogen Energy*, *34*(2), 1045–1053. https://doi.org/10.1016/j.ijhydene.2008.10.036

Knight, H. A., & Walker, R. B. (1953). The component pressure losses in combustion chambers. In *Aeronautical Research Council Reports & Memoranda*.

Lefebvre, A. H., & Ballal, D. R. (2010). Gas turbine combustion: Alternative fuels and emissions. In *Gas Turbine Combustion* (3rd ed). CRC Press. https://doi.org/10.1201/9781420086058

Lokini, P., Roshan, D. K., & Kushari, A. (2019). Influence of swirl and primary zone airflow rate on the emissions and performance of a liquid-fueled gas turbine combustor. *Journal of Energy Resources Technology*, *141*(6), 1–9. https://doi.org/10.1115/1.4042410

Mark, C. P., & Selwyn, A. (2016). Design and analysis of annular combustion chamber of a low bypass turbofan engine in a jet trainer aircraft. *Propulsion and Power Research*, *5*(2), 97–107. https://doi.org/10.1016/

j.jppr.2016.04.001
Mathys, F., Wild, P., & Wang, J. (2021). CO2 reduction measures in the aviation industry: Current measures and outlook. *International Journal of Aviation, Aeronautics, and Aerospace*, *8*(2), 1–19. https://doi.org/10.15394/ijaaa.2021.1581
Mattingly, J. D., Heiser, W. H., & Pratt, D. T. (2002). *Aircraft engine design* (2nd ed). American Institute of Aeronautics and Astronautics, Inc.
Melconian, P., & Modak, J. (1985). Combustors design. In *Saywer's Gas Turbine Engineering Hand book: Theory & Design. Vol.1*. Turbomachinery International Publications.
Mellor, A. (1990). *Design of modern turbine combustors* (1st ed). Academic.
Mohammad, B., & Jeng, S. M. (2009). Design procedures and a developed computer code for preliminary single annular combustor design. *45th AIAA/ASME/SAE/ASEE Joint Propulsion Conference and Exhibit*, *August*, 1–29. https://doi.org/10.2514/6.2009-5208
Odgers, J. (1977). Combustion modelling within gas turbine engines, some applications and limitations. *15th Aerospace Sciences Meeting, Los Angels, California, January 24-26*, 1–37. https://doi.org/10.2514/6.1977-52
Rolls Royce. (1996). *The jet engine* (5th ed). Rolls-Royce plc, Derby, England.
Saboohi, Z., Ommi, F., & Fakhrtabatabaei, A. (2016). Development of an augmented conceptual design tool for aircraft gas turbine combustors. *The International Journal of Multiphysics*, *10*(1), 53–74. https://doi.org/10.21152/1750-9548.10.1.53
Sawyer, J. (1985). *Gas turbine engineering handbook. Vol.1 theory & design* (3rd ed). Gas Turbine Publications.
Syred, N., & Beér, J. (1974). Combustion in swirling flows: A review. *Combustion and Flame*, *23*(2), 143–201. https://doi.org/10.1016/0010-2180(74)90057-1
Zhang, P., Liu, Y. P., Li, J. H., & Yan, Y. W. (2019). Design and numerical simulation of a micro-gas turbine combustor. *Journal of Applied Fluid Mechanics*, *12*(5), 1707–1718. https://doi.org/10.29252/jafm.12.05.29608